# Fast synchrotron X-ray tomography study of the packing structures of rods with different aspect ratios*

Zhang Xiao-Dan(张晓丹)[a], Xia Cheng-Jie(夏成杰)[a], Xiao Xiang-Hui(肖相辉)[b], and Wang Yu-Jie(王宇杰)[a]†

[a] *Department of Physics, Shanghai Jiao Tong University, Shanghai* 200240, *China*
[b] *X-ray Science Division, Argonne National Laboratory,* 9700 *South Cass Avenue, IL* 60439, *USA*

(Received 4 November 2013; revised manuscript received 2 December 2013; published online 20 February 2014)

We present a fast synchrotron X-ray tomography study of the packing structures of rods with different aspect ratios. Utilizing the high flux of the X-rays generated from the third-generation synchrotron source, we can complete a high-resolution tomography scan within a short period of time, after which the three-dimensional (3D) packing structure can be obtained for the subsequent structural analysis. The image phase-retrieval procedure has been implemented to enhance the image contrast. We systematically investigated the effects of particle shape and aspect ratio on the structural properties including packing density and contact number. It turns out that large aspect ratio rod packings will have wider distributions of free volume fraction and larger mean contact numbers.

**Keywords:** synchrotron X-ray imaging, tomography, rod packing structure

**PACS:** 45.70.Cc, 87.59.–e **DOI:** 10.1088/1674-1056/23/4/044501

## 1. Introduction

The packing of particles is a topic with a long standing history.[1,2] An archetypical model system for particle packing is sphere packing, which has attracted wide interest in both the theoretical[3,4] and experimental[5] community. In recent years, anisotropic particle packing[6–11] is gaining more and more attention owing to their rich behaviors associated with the extra rotational degrees of freedom as compared to spheres. To establish a statistical understanding of the granular packing structures, a detailed microscopic local structure is needed. However, this remains a challenge since three-dimensional (3D) structural information is not easily available. The utilization of X-ray tomography[12,13] is a successful solution to this problem in the study of granular packing structures owing to its penetrating power. However, even with the availability of the X-ray tomography technique, challenges remain since the data acquisition speed is normally so slow for an ordinary tomography study that a sufficient number of samples cannot be measured within a reasonable time limit. Fortunately, the utilization of the third-generation synchrotron X-ray source can drastically overcome this difficulty, which makes it possible to gain a statistically significant number of packing structures in an acceptable period of time. In the current study, we implement a fast synchrotron micro-tomography study of the anisotropic rod packing structures. Since the rods' absorption is rather weak at a relatively high energy of the "pink" X-ray beam, we introduce the phase-retrieval algorithm[14,15] to enhance the contrast of the image during the image processing steps. We then analyze the influence of the rod aspect ratio on its packing properties.

In addition, we present the details of the X-ray tomography experiment and image processing steps. We study the local packing properties including the free volume fraction and contact number to investigate the effect of aspect ratio on the packing structure.

## 2. Experimental setup

In the current study, we studied the 3D packing structures of nylon rods with aspect ratios of 0.8:1, 1.6:1, 4:1, and 5:1 respectively. The experiment was carried out at the 2BM beamline of Advanced Photon Source of Argonne National Laboratory. A fast air-bearing tomography stage was used to record the sample at different imaging angles, with 1800 projection images taken at a constant rotation speed in a course of 6 s. The distance between the object and LAG scintillator is 30 cm and the size of the projection image is 2016 (h)×1200 (v) pixels with an effective pixel size of 5.5 μm.

To fully harness the high flux X-ray beam, we utilize the full "pink" spectrum after the mirror. Since the X-ray energy used is typically in the 20-keV range, the real part difference of the complex refractive index between nylon and air is rather small, which results in a modest absorption contrast. In order to enhance the contrast between the rod and its surrounding air, we obtained the phase information by the phase-retrieval algorithm.[14,15] Then we reconstruct the three-dimensional structure using these phase retrieved projection images by the

*Project supported by the National Natural Science Foundation of China (Grant No. 11175121) and the National Basic Research Program of China (Grant No. 2010CB834301). Use of the Advanced Photon Source, an Office of Science User Facility operated for the U.S. Department of Energy (DOE) Office of Science by Argonne National Laboratory, was supported by the U.S. DOE (Grant No. DE-AC02-06CH11357).

†Corresponding author. E-mail: yujiewang@sjtu.edu.cn

© 2014 Chinese Physical Society and IOP Publishing Ltd 

ordinary filter back projection algorithm. The typical reconstructed structures of rod packing with different aspect ratios are shown in Fig. 1, and the corresponding sizes of rods are shown in Table 1. Each aspect ratio packing is repeated around thirty times to gain sufficient statistics.

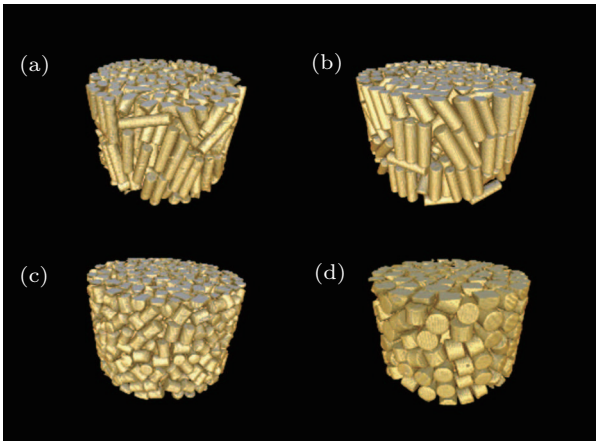



**Fig. 1.** (color online) The 3D structures of rod packing with different aspect ratios. The aspect rations are (a) 5:1, (b) 4:1, (c) 1.6:1, (d) 0.8:1.

**Table 1.** The lengths and diameters of the four types of rods studied in the experiment.

| Packing | a | b | c | d |
|---|---|---|---|---|
| Length/mm | 2.5 | 2.0 | 0.8 | 0.8 |
| Dimeter/mm | 0.5 | 0.5 | 0.5 | 1 |

## 3. Results

Extensive image segmentation efforts need to be carried out before the structural analysis. In the current study, we use the software Matlab to do image segmentation. The images are binarized using original images, then the rods are eroded until they are separated from each other. The eroded images are inverted between the background and the objects and the watershed segmentation technique is applied to the inverted images. Once the segmentation is done, the value of the parts which belonging to the background in the original binary image is multiplied by zero in obtaining the final segmented image. The whole process is carried out in three dimensions as shown in Fig. 2.

From the segmented structures, it is easy to extract the basic information of each rod, such as its volume, center, and the moment of inertia, which are useful for the analysis of packing properties in subsequent steps. The volume fraction can be calculated simply as the volume ratio of the rods and the total volume. Voronoi tessellation has been used to obtain the Voronoi cell[16] and the corresponding free volume associated with each rod. Figure 3 shows the probability distribution function of the local volume fraction $\Phi$ of rods with different aspect ratios. The volume fraction $\Phi$ is defined as the ratio between the rod's volume $V_{\rm rod}$ and the corresponding Voronoi volume $V_{\rm voro}$, $\Phi = V_{\rm rod}/V_{\rm voro}$. The corresponding mean volume fraction is 0.6446, 0.6707, 0.5732, and 0.5589 for the packings with aspect ratios of 0.8:1, 1.6:1, 4:1, and 5:1, respectively. The variance $\sigma_\Phi^2$ is 0.0019, 0.0020, 0.0033, and 0.0031 accordingly. It is obvious that packings with high aspect ratios have larger variances. These results suggest that the excluded volume effect becomes stronger as the aspect ratio increases.[17]

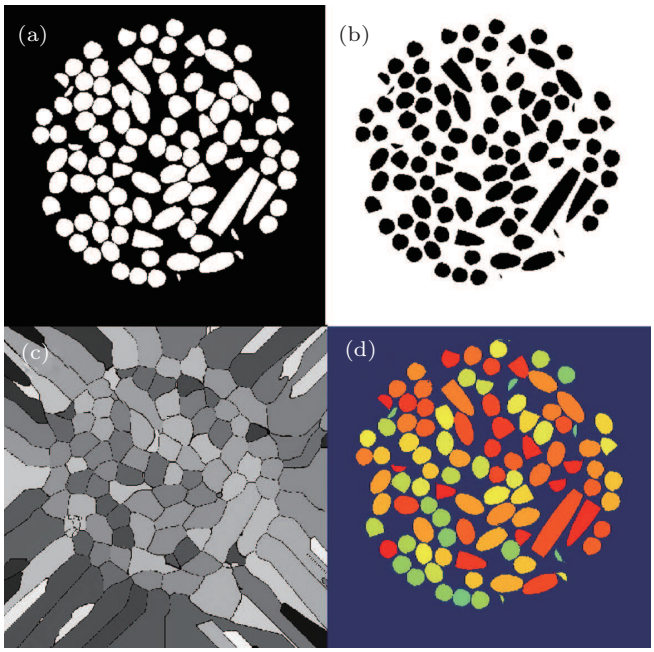



**Fig. 2.** (color online) The segmentation procedure. (a) The binary image, (b) the inverse eroded image, (c) the image obtained from 3D watershed segmentation, (d) the segmented packing structure, with each rod having a unique serial number for subsequent analysis.

In order to accurately calculate the contact number[18] for each rod, we first define a volume which contains all its potential neighbors. Then we calculate the shortest distance between the rod and its each neighbor. Next, we dilate the rod with a series of value $x$ (negative $x$ corresponds to erosion of the rod), we can obtain a series of mean contact number $Z$ as a function of $x$. The functional dependency of $Z$ on $x$ is supposed to satisfy the contact number scaling function (CNS function)[19] as

$$Z(x) = \frac{a}{2}(1+\mathrm{erf}(c(x-b))) + \theta(x-b)d(x-b). \quad (1)$$

In this function, $x$ is the dilated size, erf is the error function, $b$ is the actual diameter of the rod. $c$ is a constant and $d$ is the increased slope of CNS function when the volume of the dilated rod is larger than the actual volume, and $\theta(x-b)$ is the heaviside function. We then fit the obtained contact number $Z(x)$ with the CNS function. The fitting parameter $a$ is the mean contact number we need. The corresponding fitting results using CNS function are shown in Fig. 4. The corresponding fitting mean contact numbers are 6.54, 7.91, 7.97,

and 8.84 for aspect ratios of 0.8:1, 1.6:1, 4:1, and 5:1 respectively, as shown in the inset of the first graph of Fig. 4. We find that the contact number increases monotonically as the aspect ratio increases. This can be explained by the increased number of contacts needed to maintain mechanical stability, associated with the rotational degrees of freedom for anisotropic particles.[17,18] This is different from the sphere packing in which the rotational degrees of freedom remain inactive. The isostatic conjecture states that the mean contact number of a rod packing should be 10 since there are five degrees of freedom for each rod (three translational and two rotational).[20] Our experiment is consistent with the previous study on spherocylinders that the mean contact number rises gradually but not abruptly to 10. This has been explained by Chaikin *et al.*[21] for why the isostatic conjecture may fail for non-spherical particles.

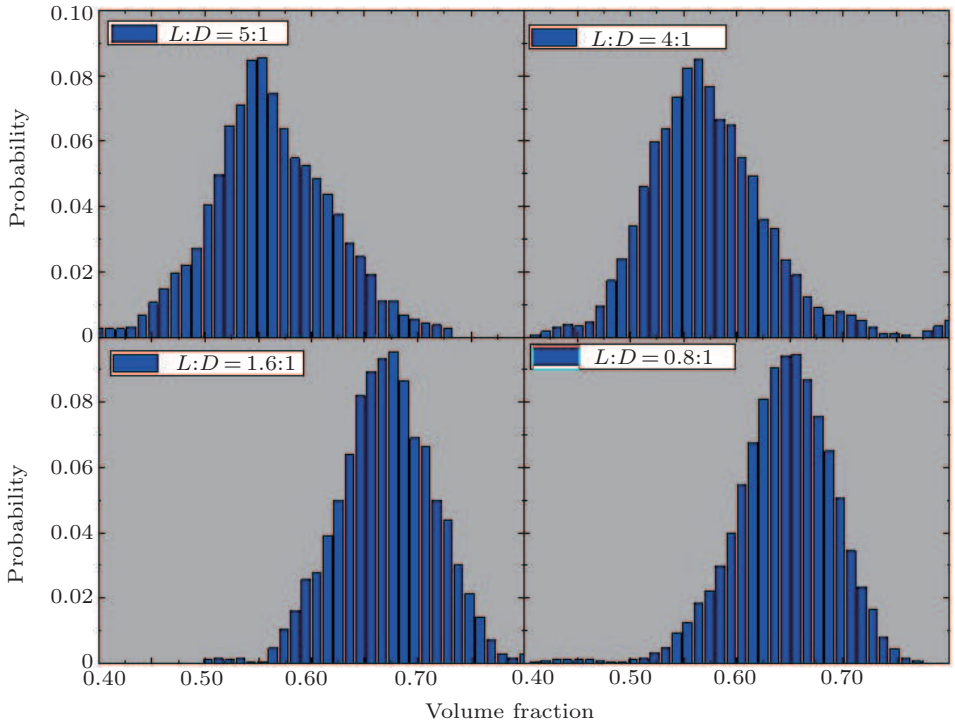



**Fig. 3.** (color online) The probability distributions of volume fraction of packing with different aspect ratios. The aspect ratios of each packing are displayed on the corner.

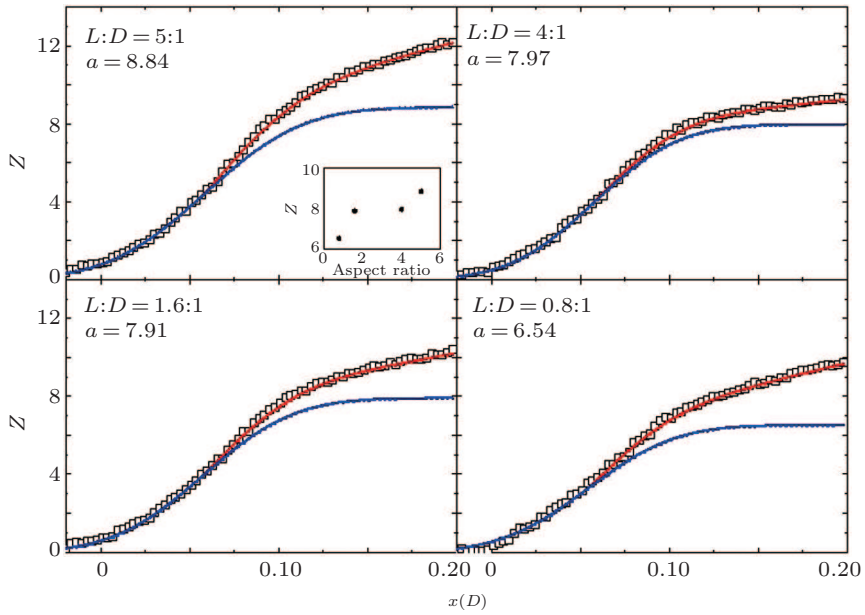



**Fig. 4.** (color online) Fitting of contact data (the black curve) using CNS function (the red curve). The blue curve is the part of error function. The fitting parameters $a$ (the mean contact number of the packing) are shown for each aspect ratio. The inset shows the relationship between the mean contact number $Z$ and the aspect ratio.

## 4. Conclusion

The utilization of the high-flux synchrotron radiation X-ray beam enables us to carry out a micron-resolution structural tomography study at significantly reduced time in comparison with regular tomography studies. Structural information of the packings is obtained from the 3D structure reconstructed using the phase retrieved projections. The free volume and mean contact number are calculated. We find that the properties of packing are strongly correlated to the shape of particles. Namely, the higher the aspect ratio is, the larger the variance of the free volume is. The mean contact number is also larger for the packing with higher aspect ratios.

## References


[1] Bernal J D 1959 *Nature* **183** 141
[2] Smith W O, Foot Paul D and Busang P F 1929 *Phys. Rev.* **34** 1271
[3] Mansfield M L, Rakesh L and Tomallia D A 1996 *J. Chem. Phys.* **105** 3245
[4] Torquato S and Stillinger F H 2010 *Rev. Mod. Phys.* **82** 2633
[5] Aste T, Saadatfar M and Senden T J 2005 *Phys. Rev. E* **71** 061302
[6] Donev A, Cisse I, Sachs D, Variano E A, Stillinger F H, Connelly R, Torquato S and Chaikin P M 2004 *Science* **303** 990
[7] Fu Y, Xi Y, Cao Y X and Wang Y J 2012 *Phys. Rev. E* **85** 051311
[8] Zhang X D, Xia C J, Sun H H and Wang Y J 2013 *AIP Conf. Proc.* **1542** 365
[9] Anita Mehta and Luck J M 2003 *J. Phys. A: Math. Gen.* **36** 365
[10] Luck J M and Anita Mehta 2003 *Eur. Phys. J. B* **35** 399
[11] Luck J M and Anita Mehta 2010 *Eur. Phys. J. B* **77** 505
[12] Aste T, Saadatfar M and Senden T J 2005 *Phys. Rev. E* **71** 061302
[13] Zhang W, Thompson K E, Reed A H and Beenken L 2006 *Chem. Eng. Sci.* **61** 8060
[14] Paganin D, Mayo S C, Gureyev T E, Miller P R and Wilkins S W 2002 *J. Microsc.* **206** 33
[15] Wang Y J, Im K S, Fezzaa K, Lee W K and Wang J, Micheli P and Laub C 2006 *Appl. Phys. Lett.* **89** 151913
[16] Danisch M, Baule A, Makse H A 2011 arXiv preprint arXiv: 1102.0608
[17] Williams S R and Philipse A P 2003 *Phys. Rev. E* **67** 051301
[18] Blouwolff J and Fraden S 2006 *Europhys. Lett.* **76** 1095
[19] Schaller F M, Neudecker M, Saadatfar M, Delaney G, Mecke K, Schröder-Turk G E and Schröter M 2013 *AIP Conf. Proc.* **1542** 377
[20] Wouterse A, Williams S R and Philipse A P 2007 *J. Phys.: Condens. Matter* **19** 406215
[21] Chaikin P M, Donev A, Man W N, Stillinger F H and Torquato S 2006 *Ind. Eng. Chem. Res.* **45** 6960